Melting of an Ice Surface in Porous Medium

M. Kazmierczak* and D. Poulikakos†
University of Illinois at Chicago, Chicago, Illinois

The buoyancy-driven flow of cold water is seriously affected by the existence of a density extremum in the vicinity of 4°C at atmospheric pressure. In this study we examine the effect of such flow on the melting of a flat ice surface inside a porous matrix. Two basic configurations are considered: a vertical flat surface and a horizontal flat surface. Interesting results document the flowfield in the liquid region. For the vertical plate configuration, depending on the water temperature far from the surface, this flow may be directed upward or downward. A regime that features local flow reversals was also identified. The effect of the flow in the melt region on the melting phenomenon (melting rate and local heat transfer) was also studied. It was found that both the flow reversals and the melting phenomenon itself reduce the local heat transfer at the melting surface.

Nomenclature

C = heat capacity
D = parameter, Eq. (15)
f = similarity function, Eq. (10)
F = similarity function, Eq. (19)
g = gravitational acceleration
k = effective thermal conductivity
K = porous medium permeability
L = latent heat of fusion
M = melting parameter, Eq. (17)
Nu = local Nusselt number
P = pressure
q = exponent in the density equation, Eq. (4)
q'' = heat-transfer rate
Ra = Darcy-modified Rayleigh number for cold water natural convection
T = temperature
u = velocity component in x direction
v = velocity component in y direction
x = coordinate parallel to melting surface
y = coordinate normal to melting surface
α = effective thermal diffusivity of porous medium
β = coefficient of thermal expansion
γ = inclination angle
η = similarity variable
θ = dimensionless temperature, Eq. (11)
Θ = dimensionless temperature, Eq. (20)
μ = fluid viscosity
ν = fluid kinematic viscosity
ξ = similarity variable
ρ = density
ψ = streamfunction

Subscripts

f = fluid region
m = melting point
o = frozen (solid) region
r = pertaining to the density maximum
∞ = freestream condition
$*$ = pertaining to horizontal surface configuration

Superscript

$'$ = derivatives with respect to η or ξ

Received June 17, 1987; revision received October 2, 1987.

*Graduate Student, Department of Mechanical Engineering.
†Associate Professor, Department of Mechanical Engineering.

I. Introduction

In the mathematical modeling of buoyancy-driven convection, it is customarily assumed that the linear Boussinesq approximation holds. According to this approximation, the fluid density is constant everywhere except in the buoyancy term of the momentum equation, where it depends linearly on temperature. There exist, however, a few fluids that feature an extremum in their density-temperature relationship. These fluids are exemplified by molten bismuth, gallium, tellurium and, most importantly, water. For water, this density extremum occurs in the vicinity of 4°C at atmospheric pressure.

The problem of cold water natural convection in porous media has received little attention, unlike its counterpart in classical fluids, which has constituted the focus of several studies over the past few decades. Ramilison and Gebhart[1] have reported theoretical results for the problem of boundary-layer, buoyancy-driven flow past a vertical plate in porous medium saturated with cold, pure or saline water. Poulikakos[2] and Blake et al.[3] considered the problem of natural convection of cold water in a rectangular layer filled with porous medium differentially heated in the horizontal[2] or vertical direction.[3] With the help of numerical simulations, these authors showed that the density extremum had a paramount effect in the cellular flow pattern in the system. A linear stability analysis for the onset of convection in a porous medium containing a liquid with a density maximum was reported by Sun and Tien.[4] Laboratory experiments verifying and extending the theoretical findings in Ref. 4 were performed by Yen.[5]

The proximity of the temperature of 4°C to the freezing point of water (0°C) makes it obvious that the water density extremum may seriously affect natural convection phenomena associated with freezing or melting processes.[6] The present study focuses on the effect of buoyancy-driven flow on the melting of a flat ice surface in porous medium. In addition to its importance from a fundamental standpoint, the present study finds applications in the melting of permafrost, the conservation of thermal energy in ice-storage units, the flow of cold water in solid matrix heat exchangers, and the food industry. Two basic configurations are examined thoroughly in the present study, namely, a vertical plate and a horizontal plate. In both configurations, the presence of the density extremum significantly alters the structure of the buoyancy-driven flow and, therefore, the melting phenomenon.

II. Mathematical Formulation

The configurations of interest are shown schematically in Fig. 1. Figures 1a and 1b pertain to the vertical melting ice

surface and Fig. 1c to the horizontal surface. We adopt the usual practice in boundary-layer analysis in designating x as the coordinate along the ice-water interface and y the coordinate normal to the interface. Since the solid boundary is gradually receding, the coordinate system is time-dependent. However, in the limit of the slow melting rate, it is reasonable to consider the melting process quasisteady.[7-10] The temperature of the interface, T_m, is the melting temperature of the ice (0°C) occupying the porous matrix. The water far from the melting front is maintained at constant temperature T_∞ ($T_\infty > T_m$). The temperature of the solid far from the melting front is also constant, T_o ($T_o < T_m$). The temperature corresponding to the water density extremum at atmospheric pressure, T_r, lies within the region $T_m < T_r < T_\infty$ for a part of the study. Cases for which $T_m < T_\infty < T_r$ are also considered.

The fluid flow in the liquid phase is governed by the Darcy flow model.[11] This model is simple and works well for flows inside homogeneous densely packed porous matrices. In the present problem, we model the melting of a flat interface in an unbounded porous medium. Therefore, we do not have solid boundaries present to cause packing imperfections in the porous medium and make the validity of the Darcy model questionable. In addition, it is assumed that the porous matrix and the liquid and solid phases are in local thermal equilibrium even in the presence of melting. This assumption has been used successfully by previous investigators.[7] It is worth noting, however, that the issue of local thermal equilibrium in phase change problems needs to be addressed in future theoretical and experimental studies. The physical properties of the porous medium, the ice and the water, are isotropic and homogeneous. Based on the given assumptions, the governing equations for the liquid region in which the buoyancy-driven flow is present are

$$\nabla \cdot \boldsymbol{v} = 0 \tag{1}$$

$$\boldsymbol{v} = \frac{K}{\mu}(-\nabla P + \rho \boldsymbol{g}) \tag{2}$$

$$\boldsymbol{v} \cdot \nabla T = \alpha \nabla^2 T \tag{3}$$

In these equations, $\boldsymbol{v}$ is the velocity vector, $\boldsymbol{v} = u\boldsymbol{i} + v\boldsymbol{j}$. As shown in Fig. 1, the velocity vector has two components: u in the x direction and v in the y direction. Since the coordinate system is fixed at the melting interface,[7,9] it appears as if the frozen porous medium moves toward the stationary melting ice/water interface with constant velocity equal to the melting velocity $v(x,0)$. The temperature is denoted by T, the pressure by P, the water density by ρ, the water viscosity by μ, the effective thermal diffusivity by α, and the permeability by K.

According to the Boussinesq approximation, the water density is assumed constant everywhere except in the buoyancy term of the momentum equation. In the vicinity of the density extremum, the usual linear density-temperature relationship is not appropriate. Of the several alternative relationships proposed and used by various investigators,[3-5,12,13] we chose to use the most recent one, proposed by Gebhart and Mollendorf.[13] It holds for a rather large temperature range (between 0° and 20°C), it is simple, and it appears to be at least as accurate as any other density/temperature relationship for the region of the density extremum of water. This relationship reads

$$\rho = \rho_r\left(1 - \beta|T - T_r|^q\right) \tag{4}$$

where subscript r denotes the density maximum, $T_r = 4.02932$°C, $\rho_r = 999.972$ kg/m^3, $\beta = 9.297173 \times 10^{-6} C^{-q}$, and $q = 1.894816$. Because of the form of Eq. (4), it is possible that the buoyancy-induced flow may be directed parallel (Fig. 1a) or opposite (Fig. 1b) to the gravity vector. In addition, local flow reversals have been observed both in classical fluids[14] and in porous media.[1]

Figure 2 reports diagrammatically the different flow regimes that may result for the vertical surface configuration, depending on the value of the temperature of the warm stationary fluid that initiates the melting phenomenon. It is understood that the melting surface is at 0°C. Flow reversal is possible when the main flow in the melt is directed both upwards and downwards. More details regarding the flow regimes will be discussed in later sections.

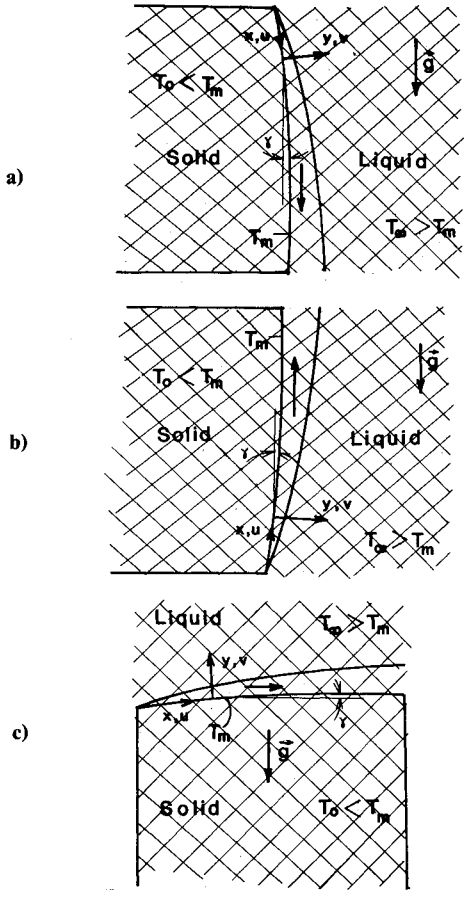

Fig. 1 Schematic of the melting of a flat ice surface in porous medium in the presence of natural convection: a) vertical surface, downflow; b) vertical surface, upflow; and c) horizontal surface.

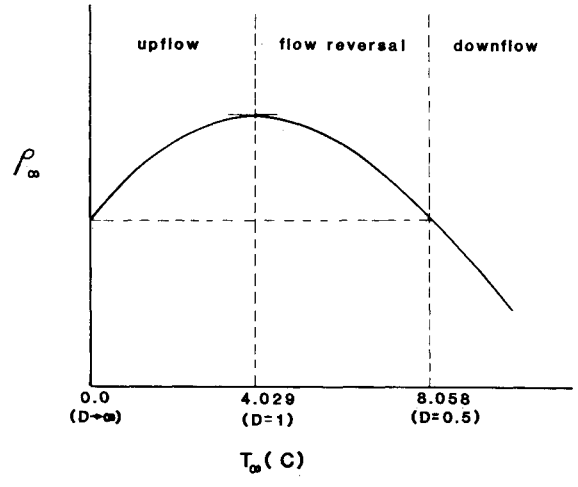

Fig. 2 The dependence of the density of the ambient water on temperature in the vicinity of the density extremum, and the different possible flow regimes. The figure is drawn diagrammatically and not to scale.

The boundary conditions necessary to complete the problem formulation are

$$y=0:\ T=T_m,\qquad k\frac{\partial T}{\partial y}=\rho[L+C_s(T_m-T_o)]v \quad (5)$$

$$y\to\infty:\ u\to 0, T\to T_\infty \quad (6)$$

where k is the water thermal conductivity, L the latent heat of fusion, and C_s the heat capacity of the solid.

The first of the two boundary conditions on the melting front ($y=0$) simply states that the interface temperature equals the ice melting temperature. The second condition at $y=0$ is a direct result of an energy balance. It states that the heat conducted to the melting surface is equal to the heat of melting plus the sensible heat required to raise the temperature of the ice T_o to its melting temperature T_m.[7-9] Transient effects in the solid have been neglected. As discussed in Refs. 7–9, this assumption is appropriate as long as the melting body is large compared to its thermal boundary-layer thickness. The boundary conditions at infinity are self-evident.

In the present analysis, we shall assume that the inclination angle γ (Fig. 1) of the melting surface is small, following Chen et al.,[10] and Epstein and Cho,[7,9] therefore,

$$\cos\gamma \simeq 1+0(\gamma^2) \quad (7)$$

If the vector equation (2) is written in Cartesian coordinates, the x component of this equation will contain a body force term of magnitude $\rho g\cos\gamma$. Although x is measured along the surface of the melting ice, which may not necessarily form a perfectly vertical (Figs. 1a and 1b) surface, the preceding assumption allows us to replace $\cos\gamma$ by unity in the momentum equation with only second-order error. Similar discussion holds for the horizontal surface (Fig. 1c). Based on this approximation, the equations for both the vertical and the horizontal configurations admit similarity solutions. The details for the formulation of the similarity problem are outlined in the next section.

III. Similarity Solution

In boundary-layer flows, only the momentum equation in the direction parallel to the boundary is relevant. In addition, several simplifying assumptions render the governing equations more manageable mathematically. These assumptions are textbook material[15] and will not be repeated here for brevity. The similarity equations for each configuration will be discussed separately.

Vertical Surface

Introducing the streamfunction in the usual manner

$$u=\frac{\partial\psi}{\partial y} \quad (8)$$

$$v=-\frac{\partial\psi}{\partial x} \quad (9)$$

we assume next that the dimensionless temperature and the dimensionless streamfunction have the following functional form:

$$\psi=\alpha Ra^{1/2}f(\eta) \quad (10)$$

$$\theta=\frac{T-T_m}{T_\infty-T_m} \quad (11)$$

where η is the similarity variable

$$\eta=Ra^{1/2}\frac{y}{x} \quad (12)$$

and Ra is the Darcy-modified Rayleigh number appropriate for cold water natural covection,

$$Ra=\frac{Kg\beta|T_\infty-T_m|^q x}{\nu\alpha}$$

After the usual algebraic manipulations, the similarity boundary-layer momentum and energy equations read

$$f''=\pm\left(|\theta-D|^q\right)' \quad (13)$$

$$\theta''+\tfrac{1}{2}f\theta'=0 \quad (14)$$

where parameter D is defined as

$$D=\frac{T_r-T_m}{T_\infty-T_m} \quad (15)$$

and the primes denote differentiation with respect to the similarity variable η. The plus sign in Eq. (13) refers to the upward flow configuration (Fig. 1b) and the minus sign to the downward flow configuration (Fig. 1a).

Parameter D is of paramount importance in the present problem, for it places the temperature of melting interface (T_m) and the temperature of the warm fluid far from the interface (T_∞) with respect to the temperature corresponding to the water density extremum (T_r). Depending on the value of D (representing the density maximum effect), upflow, downflow, or flow reversal may occur in the melt region (Fig. 2). For example, based on Eq. (15), values of D greater than unity ($T_r-T_m>T_\infty-T_m$) imply that the flow in the melt region is directed upward (opposite to the direction of gravity).

The boundary conditions after the similarity transformation are

$$\theta(0)=0,\qquad \theta(\infty)=1,\qquad f(0)+2M\theta'(0)=0,$$
$$f'(\infty)=0 \quad (16)$$

The melting parameter M is defined as

$$M=\frac{C_f(T_\infty-T_m)}{L+C_s(T_m-T_o)} \quad (17)$$

In the preceding equation, C_f is the heat capacity of the fluid. The remaining quantities have been defined earlier.

The numerical solution of Eqs. (13), (14), and (16) was performed based on a double-shooting scheme involving the fourth-order Runge-Kutta method.[16] To start the numerical integration, $\theta'(0)$ and $f'(0)$ were guessed. Next, Eqs. (13) and (14) were integrated simultaneously in η and the values of θ and f' at infinity were checked. The values of $\theta'(0)$ and $f'(0)$ were adjusted systematically, and the integration process was repeated until the conditions $\theta(\infty)=1$ and $f'(\infty)=0$ were satisfied.

Horizontal Surface

Following the given procedure, the similarity functions for the horizontal plate geometry are introduced:

$$\xi=Ra^{1/3}(y/x) \quad (18)$$

$$\psi_*=\alpha Ra^{1/3}F(\xi) \quad (19)$$

$$\Theta(\xi)=\frac{T-T_m}{T_\infty-T_m} \quad (20)$$

Using the preceding definitions, we arrive at the following similarity boundary-layer momentum and energy equations

$$F''=\pm\tfrac{2}{3}\left\{\xi\left\{|\Theta-D|\right\}^q\right\}' \quad (21)$$

$$\Theta'' + \tfrac{1}{3}F\Theta' = 0 \qquad (22)$$

The plus sign in the momentum equation (21) corresponds to the case where the melt is located above the solid (Fig. 1c). Only this case will be investigated in this study, for brevity. The minus sign in Eq. (21) corresponds to the case where the melt is on the underside of the solid. The corresponding boundary conditions are

$$\Theta(0) = 0, \quad \Theta(\infty) = 1, \quad F'(\infty) = 0$$
$$F(0) + 3M\Theta'(0) = 0 \qquad (23)$$

In the equations pertinent to the horizontal plate configuration, the primes denote differentiation with respect to ξ.

The procedure for the numerical solution of Eqs. (21–23) is similar to the procedure used to integrate numerically Eqs. (13), (14), and (16) for the vertical plate configuration. The double-shooting scheme again requires the guessing of $\Theta'(0)$ and $F'(0)$ to start the numerical integration via the fourth-order Runge-Kutta method. After systematic adjustments of the guessed values and repetitions of the numerical integration, the solution to the problem, which satisfies the boundary conditions at infinity in Eq. (23), is obtained.

Of practical significance is the calculation of the melting rate (local heat flux) at the ice/water interface. This result will illustrate the effect of the presence of the buoyancy-driven flow on the melting front. The calculation of the melting rate is performed and reported with the help of the local Nusselt number:

$$Nu = \frac{q''x}{k(T_\infty - T_m)} = \begin{cases} \theta'(0)\,Ra^{1/2} & \text{(vertical plate)} \\ \Theta'(0)\,Ra^{1/3} & \text{(horizontal plate)} \end{cases} \qquad (24)$$

The melting velocity of the interface depends on x and is given by the following simple equation:

$$v(x,0) = \frac{\alpha}{x} MNu \qquad (25)$$

Equation (25) was derived by combining Eqs. (5) and (24). Clearly, for prescribed values of M and D, once $\theta'(0)$ or $\Theta'(0)$ have been obtained, the velocity of the melting ice/water interface can be determined directly from Eq. (25). This velocity is proportional to $x^{-2/3}$ for the horizontal plate configuration. Based on this fact, the melting process is faster near the "leading edge" of the interface where the "warm" ambient water comes for the first time into direct contact with the cold melting ice front.

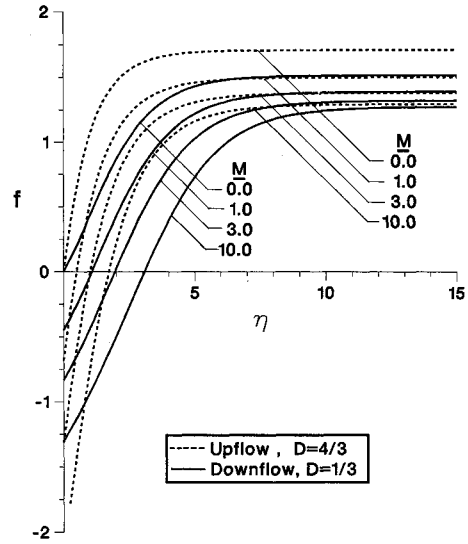

Fig. 3 The dependence of the streamfunction f on the melting parameter M for the vertical surface configuration for a typical upflow ($D = \frac{4}{3}$) and a typical downflow ($D = \frac{1}{3}$) case.

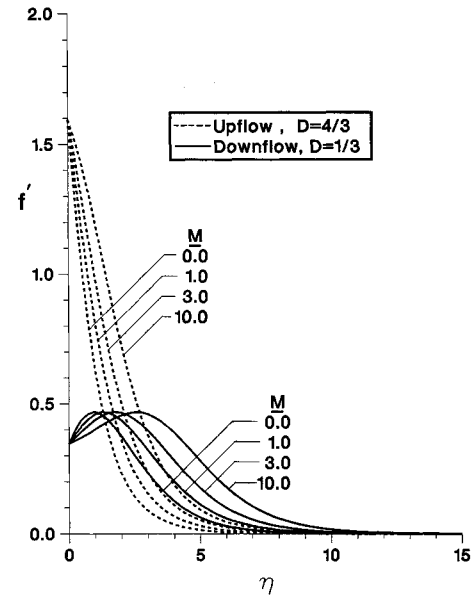

Fig. 4 The dependence of the x component of velocity, f', on the melting parameter M for the vertical surface configuration for a typical upflow ($D = \frac{4}{3}$) and a typical downflow ($D = \frac{1}{3}$) case.

IV. Results and Discussion

At first, results were obtained for the vertical plate configuration pertinent to cases where the flow inside the boundary layer formed by the melt is directed only upward or only downward (Figs. 1a, 1b, and 2), i.e., no flow reversal is present in the system. In Figs. 3 and 4, the effect of the problem parameters on the flowfield is depicted. For a fixed value of D, increasing the melting parameter M decreases the dimensionless streamfunction f (Fig. 3). The dependence of f on η resembles that for natural convection from a vertical plate in the presence of blowing at the plate. Increasing the value of parameter D from $\frac{1}{3}$ to $\frac{4}{3}$ has a dramatic effect on the flowfield: the flow direction is altered by 180°. This fact is shown clearly in Fig. 4, which reports results for the velocity component parallel to the melting plate. This behavior is due to the existence of the density extremum for water at $D = 1$ as explained earlier. The presence of a peak in the velocity distribution for the downflow case is because of the chosen value of $D = \frac{1}{3}$. This value of D implies that the temperature corresponding to the density extremum is in the region $T_m < T_r < T_\infty$. Therefore, the water at this temperature sinks the fastest. On the other hand, in the upflow case, $T_m < T_\infty < T_r$ ($D = \frac{4}{3}$), the density and the velocity decrease monotonically with increasing η. In the downflow case, increasing M shifts the location of velocity maximum away from the melting interface. This result makes sense physically if it is realized that the melting phenomenon acts as a blowing boundary condition at the wall. Consequently, more intense melting (increasing M) tends to thicken the boundary layer and move the location of the velocity maximum away from the plate. The thickening of the boundary layer with increasing M is also evident in the upflow case in Fig. 4.

Representative results for the temperature variation in the melt layer in the absence of flow reversal are shown in Fig. 5. In both the upflow and the downflow cases, the value of the temperature increases monotonically from T_m ($\theta = 0$) at the plate to T_∞ ($\theta = 1$) at infinity. As the melting parameter

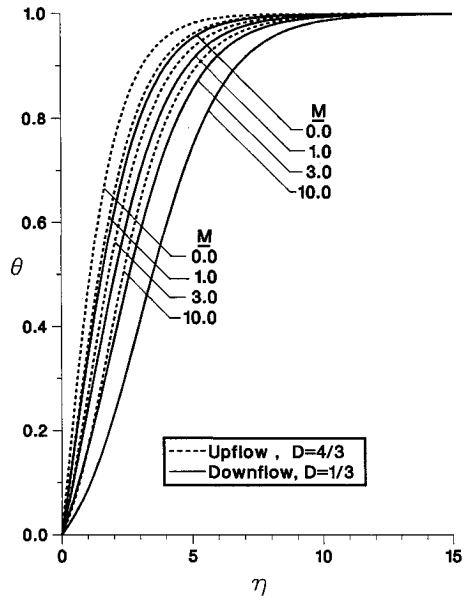

Fig. 5 The dependence of the temperature θ on the melting parameter M for the vertical plate configuration for a typical upflow ($D = \frac{4}{3}$) and a typical downflow ($D = \frac{1}{3}$) case.

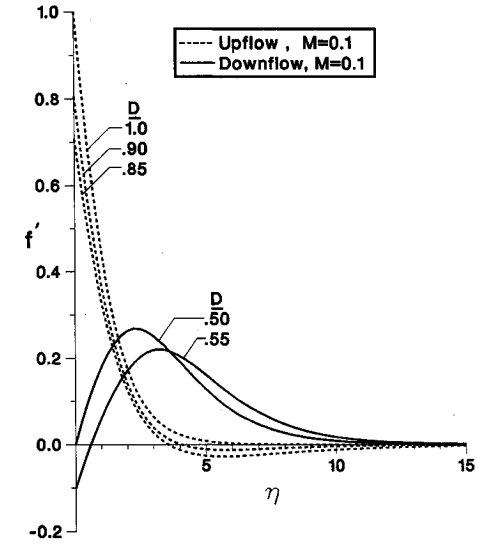

Fig. 6 The dependence of the x component of velocity, f', on parameter D for the vertical plate configuration when flow reversal is present. Examples are shown where the main flow is upward and downward.

increases, the temperature for a fixed value of η decreases and the thermal boundary layer thickens.

Figures 6 and 7 pertain to cases where flow reversal does exist in the system. It is worth noting that local flow reversal occurs across the layer where the buoyancy force changes sign, since Eq. (13) implies that the velocity parallel to the melting surface is proportional to the buoyancy force. In terms of values of parameter D, it can be easily shown that flow reversal occurs in the region $0.5 < D < 1$. As shown in Fig. 6, when the main flow is downward, the reversal region is located near the plate. When the main flow is upward, the flow reversal occurs away from the melting surface and near the vicinity of the edge of the boundary layer. Similar results were obtained by Ramilison and Gebhart[1] in the limit of no melting. Regarding the temperature distribution in the melt (Fig. 7), it appears that in both cases (upward and downward

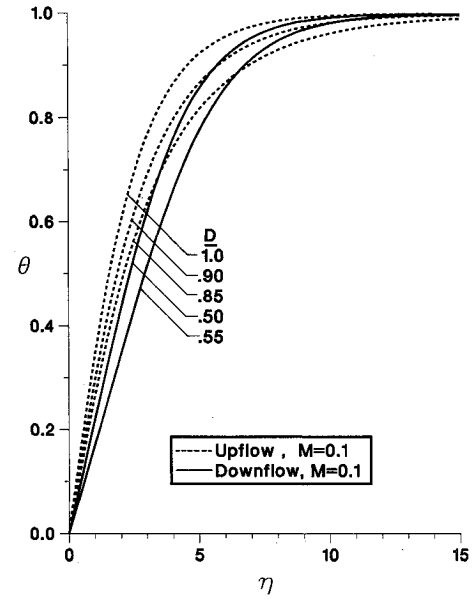

Fig. 7 The temperature variations in the melt for the velocity fields (containing flow reversals) shown in Fig. 6.

main flow) the presence of the flow reversal thickens the thermal boundary layer.

It was observed that the existence of a local flow reversal made the convergence of the numerical solution slow. This fact became more obvious as the value $D = 0.57$ was approached by gradually increasing the value of D starting from $D = 0.5$. The same was true when the value $D = 0.83$ was approached by gradually decreasing the value of D starting from $D = 1$. Convergence was not possible for values of D in the range $0.57 < D < 0.83$ where the flow reversals were significant. Similar difficulties with numerical convergence in the presence of flow reversal have been reported by other investigators.[1]

Another question that needs clarification pertains to the validity of the boundary-layer approximations in the presence of flow reversal. These approximations are valid provided that the changes of the problem variables (such as velocity) in the direction parallel to the plate (x) are small compared to the changes of the problem variables in the direction perpendicular to the plate (y). Based on simple scaling arguments, it can be shown[1] that

$$\frac{0(u)}{0(v)} \sim 0(Ra)^{1/2} \tag{26}$$

$$\frac{0(y)}{0(x)} \sim 0(Ra)^{-1/2} \tag{27}$$

From this, for a given set of physical parameters, the flow reversal solutions produced by the present analysis are accurate if Eqs. (26) and (27) are satisfied.

The impact of the melting parameter M on the local heat-transfer rate to the melting surface is summarized in Fig. 8 with the help of the Nusselt number defined in Eq. (24) for a typical upflow and typical downflow case. It so happens that the two cases shown in Fig. 8, the upflow case ($D = \frac{4}{3}$) yields higher values of Nu than the downflow case ($D = \frac{1}{3}$). Increasing M decreases the local heat transfer significantly. As discussed before in connection with Figs. 3–5, the melting phenomenon acts like a "blowing" condition at the plate. It thickens the thermal boundary layers and is responsible for the decrease in Nu shown in Fig. 8. At small values of M a plateau is reached. This plateau features the maximum value of Nu corresponding to the case of no melting. Also shown in Fig. 8 are the values reported graphically in Ref. 1 for the case

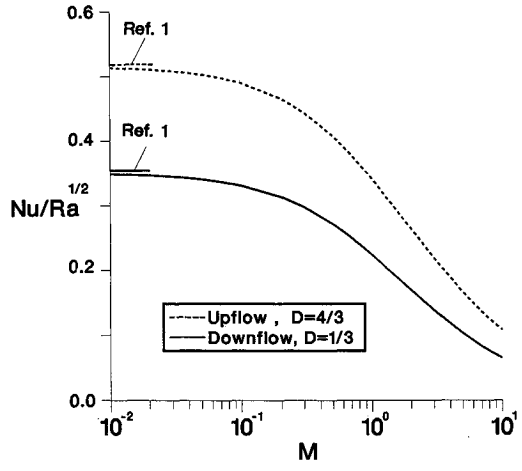

Fig. 8 The effect of the melting parameter M on the heat transfer rate for the vertical plate configuration for a typical upflow ($D = \frac{4}{3}$) and a typical downflow ($D = \frac{1}{3}$) case.

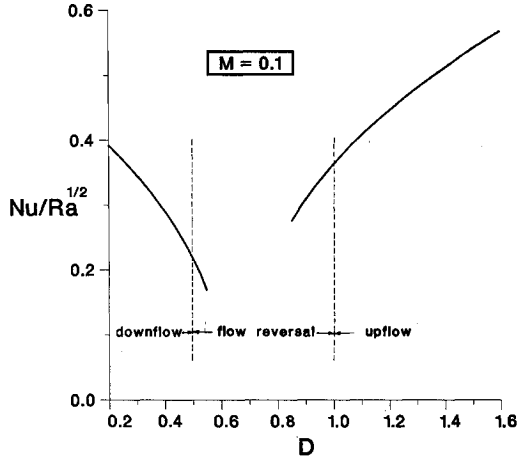

Fig. 9 The dependence of the heat transfer rate on parameter D for the vertical plate configuration.

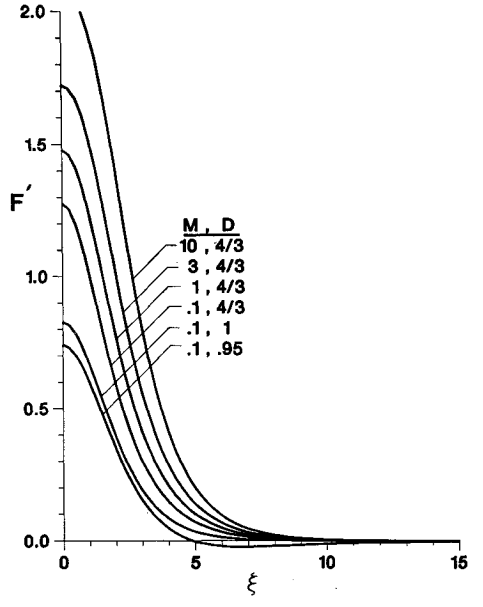

Fig. 10 The dependence of the x component of velocity, F', on the melting parameter M for the horizontal plate configuration for representative values of D.

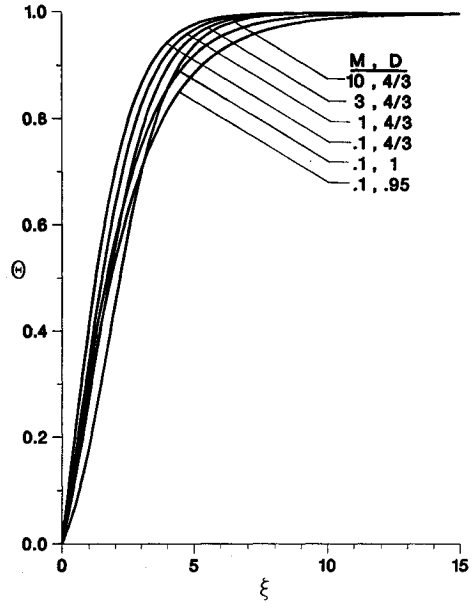

Fig. 11 The dependence of the temperature Θ on the melting parameter M for the horizontal plate configuration for representative values of D.

of no melting ($M = 0$). Clearly, as M decreases, the values of Nu obtained in the present study approach those reported in Ref. 1.

The effect of parameter D on Nu is shown in Fig. 9. There is a drastic drop in the value of Nu as the flow reversal region is approached from either side. Moving away from the flow reversal region yields significant heat-transfer enhancement for both the upflow and the downflow cases. The detrimental effect that the flow reversal has on Nu is a direct result of the thickening of the thermal boundary layer caused by the flow reversal as discussed in connection with Fig. 7.

The main results obtained for the horizontal plate configuration are shown in Figs. 10–13. It is worth noting that since the "cold" solid is positioned under the "warm" fluid, the buoyancy-driven flow exists solely because of the presence of the density extremum. If the density-temperature relationships were linear, the system would be stably stratified and no flow motion would take place. The configuration in Fig. 1c is then a powerful example of the important role the density extremum has in the melting process.

The dependence of F' and Θ on the melting parameter M and the similarity variable ξ (Figs. 10 and 11) is similar qualitatively to that discussed following Figs. 4 and 5 relevant to the vertical plate configuration. For brevity, this discussion will not be repeated here. The dependence of Nu on M (Fig. 12) proves that the melting phenomenon inhibits natural convection heat transfer from the liquid to the solid in the horizontal plate configuration as well. Unlike in Fig. 8, we cannot compare the results of Fig. 12 in the limit of no melting ($M \to 0$) to published results of other investigators for natural convection of cold water from a horizontal plate in a porous medium. The reason for this is that to the best of our knowledge, such results do not exist in the open literature. The effect of parameter D on the heat transfer is drastic (Fig. 13). In a manner similar to the vertical plate configuration, flow reversals were observed for a certain range of values of parameter D. When this happened, a reduction in the local heat-transfer rate was observed. In addition, the convergence of the numerical solution became very slow and difficult to attain. No solutions were obtained in the region $0.7 < D < 0.95$.

V. Conclusion

In this study, the effect of the flow of cold water driven by thermal buoyancy on the melting of a flat ice surface em-

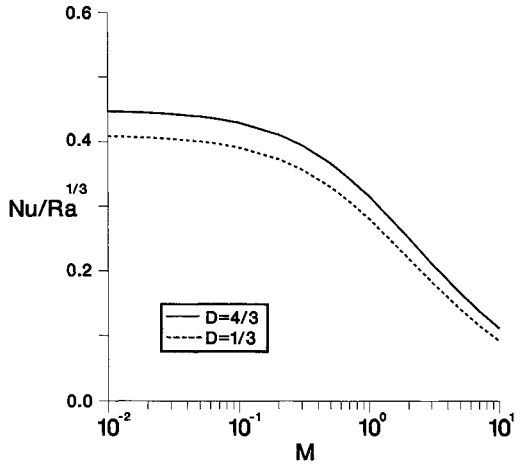

Fig. 12 The effect of the melting parameter M on the heat transfer rate for the horizontal plate configuration for representative values of D.

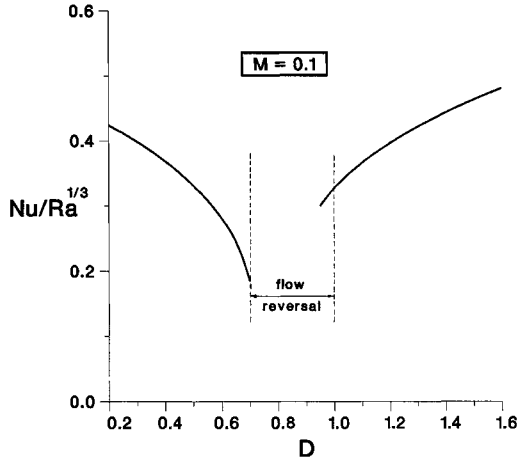

Fig. 13 The dependence of the heat transfer rate on parameter D for the horizontal plate configuration.

bedded inside a porous matrix was investigated. The melting interface was placed either vertically (parallel to the gravity vector) or horizontally. In both cases, it was demonstrated that the presence of the density extremum of water associated with the temperature of 4°C had a drastic effect on the flow and temperature fields in the melt layer. Depending on the value of the temperature of the ambient fluid (represented by parameter D), the flow in the melt was directed upward or downward. For a certain region of values of D, flow reversals were observed. The flow reversals as well as the melting phenomenon itself (parameter M) reduced the local heat transfer to the melting surface.

In summary, the effect of the buoyancy-driven flow of cold water on melting in porous media needs careful examination, for it can seriously affect or even dominate the melting process. The presence of the density extremum renders the flow in the melt considerably more interesting and more difficult to predict compared to natural convection flows in fluids in which the density-temperature relationship is linear.

Acknowledgment

Support for this research, provided by NSF through Grant CBT-84-51144, is greatly appreciated.

References

[1]Ramilison, J.M. and Gebhart, B., "Buoyancy Induced Transport in Porous Media Saturated with Pure or Saline Water at Low Temperatures," *International Journal of Heat and Mass Transfer*, Vol. 23, 1980, pp. 1521–1530.

[2]Poulikakos, D., "Maximum Density Effects on Natural Convection in a Porous Layer Differentially Heated in the Horizontal Direction," *International Journal of Heat and Mass Transfer*, Vol. 27, 1984, pp. 2067–2075.

[3]Blake, K.R., Bejan, A., and Poulikakos, D., "Natural Convection Near 4°C in a Water Saturated Porous Layer Heated from Below," *International Journal of Heat and Mass Transfer*, Vol. 27, 1984, pp. 2355–2364.

[4]Sun, Z.S. and Tien, C., "Onset of Convection in a Porous Medium Containing Liquid with a Density Maximum," *Heat Transfer 1970*, Vol. 4, 1970, pp. 160–165.

[5]Yen, Y-C., "Effects of Density Inversion on Free Convective Heat Transfer in Porous Layer Heated from Below," *International Journal of Heat and Mass Transfer*, Vol. 17, 1974, pp. 1349–1356.

[6]Tankin, R.S. and Farhadieh, R., "Effects of Thermal Convection Currents on Formation of Ice," *International Journal of Heat and Mass Transfer*, Vol. 14, 1971, pp. 953–961.

[7]Epstein, M. and Cho, D.H., "Melting Heat Transfer in Steady Laminar Flow over a Flat Plate," *Journal of Heat Transfer*, Vol. 98, 1976, pp. 531–533.

[8]Roberts, A.L., "On the Melting of a Semi-Infinite Body Placed in a Warm Stream of Air," *Journal of Fluid Mechanics*, Vol. 4, 1958, pp. 505–528.

[9]Epstein, M. And Cho, D.H., "Laminar Film Condensation of a Vertical Melting Surface," *Journal of Heat Transfer*, Vol. 98, 1976, pp. 108–113.

[10]Chen, M.M., Farhadieh, R., and Baker, L., "On Free Convection Melting of a Solid Immersed in a Hot Dissimilar Fluid," *International Journal of Heat and Mass Transfer*, Vol. 29, 1986, pp. 1087–1093.

[11]Cheng, P., "Heat Transfer in Geothermal Systems," *Advances in Heat Transfer*, Vol. 14, 1979, pp. 1–105.

[12]Goren, S.L., "On Free Convection in Water at 4°C," *Chemical Engineering Sciences*, Vol. 21, 1966, pp. 515–518.

[13]Gebhart, B. and Mollendorf, J.C., "A New Density Relation for Pure and Saline Water," *Deep Sea Research*, Vol. 24, 1977, pp. 831–841.

[14]Gebhart, B. and Mollendorf, J.C., "Buoyancy-Induced Flows in a Liquid Under Conditions in which a Density Extremum May Arise," *Journal of Fluid Mechanics*, Vol. 89, 1978, pp. 673–707.

[15]Schlichting, H., *Boundary Layer Theory*, 7th ed., McGraw-Hill, New York, 1979.

[16]Ferziger, J.H., *Numerical Methods for Engineering Applications*, Wiley, New York, 1981.